The Textures of Rocks in the Earth's Deep Interior: Part I. Understanding Anisotropy and Textures in Earth Materials

1. Introduction

Preferred orientation of crystallites (or texture) is an intrinsic feature of metals, ceramics, polymers, and rocks and has an influence on physical properties such as strength, electrical conductivity, wave propagation, particularly the anisotropy of properties. The directional characteristics of many polycrystalline materials were first recognized not in metals but in rocks and were described as "texture" (Omalius d'Halloy 1833). In the twentieth century texture research was largely pursued by metallurgists but recently it has gained importance in ceramics (e.g., high-temperature superconductors), polymers, and renewed interest is coming from earth sciences. The reason for the latter is that seismologists have discovered anisotropic wave propagation in large sectors of the Earth's interior and a likely cause is preferred orientation of crystals that developed by deformation during the Earth's long history. This review will highlight some aspects of textures relevant to Earth sciences. The first part introduces some special methods used by geologists and compares them with those of metallurgists. A second part will investigate anisotropy in different parts of the deep earth and explore how it can be related to texturing. Compared to metallurgists who are engaged in texture research to predict materials with favorable properties, geologists and geophysicists are using textures to interpret the past. The rationale is thus reversed. Also, the main evidence is indirect. Contrary to metals where specimens are readily available for analysis, and theories can be tested with experiments, deep Earth materials do not occur on the surface and many are unstable at ambient conditions. Yet, in spite of these differences, methods and approaches are remarkably similar, though the objects of interest vary greatly in dimension.

The Earth is divided into several major units: the crust, upper mantle, lower mantle, liquid outer core and solid inner core. Much is known about the crust, and deformational features are studied by structural geologists in great detail. Occasionally, samples from the upper mantle are juxtaposed with the crust and can be studied directly. The deeper parts remain more enigmatic. Phase relations are investigated with diamond anvil cell experiments or first principles calculations, but, for example, for the inner core, exact composition and phases are still debated. Since the Earth is not a static material but a complex dynamic system that evolves with time, deformation plays a crucial part and plastic processes that lead to texture are receiving increasing attention.

Preferred orientation in rocks has been the central subject of the classic book of Sander (1950), and since then there have been newer books on the subject (e.g., Wenk 1985, Kocks *et al.* 2000, Karato and Wenk 2002).

2. Measurements of Textures

Interpretation of textures has to rely on a quantitative description of orientation characteristics. Two types of preferred orientations are distinguished: the *lattice preferred orientation (LPO)* or "texture" (also "preferred crystallographic orientation") and the *shape preferred orientation (SPO)* (or "preferred morphological orientation"). Both can be correlated, such as sheet silicates with a flaky morphology in schists. In many cases they are not. In a metamorphic quartzite the grain shape depends on deformation rather than on crystallography.

Geologists use many methods to determine preferred orientation. With the petrographic microscope equipped with a universal stage, the orientation of individual grains can be measured in thin sections (e.g., Phillips, 1991). Today, diffraction techniques are most widely used to measure LPO of rocks as well as of metals (e.g., Bunge 1986, Snyder *et al.* 1999). X-ray diffraction with a pole figure goniometer is a routine method. Neutron diffraction offers some distinct advantages, particularly for large bulk samples. Electron diffraction using the transmission (TEM) or scanning electron microscope (SEM) has become a popular technique. As we will see, for *in situ* experiments at high pressure, synchrotron x-rays provide unique opportunities.

With the pole-figure goniometer (Schulz 1949), incomplete pole figures are measured, usually in reflection geometry. From several pole figures of different lattice planes the orientation distribution function (ODF) is derived. Minerals in rocks are often coarse grained and surfaces over which a pole figure goniometer averages may not be statistically representative.

With neutron diffraction of high penetration and low absorption, large sample volumes (1–10 cm diameter) can be measured. Intensity corrections are generally unnecessary and complete pole figures can be determined in a single scan. A conventional neutron texture experiment at a reactor neutron source uses monochromatic radiation produced with single-crystal monochromators. Another method is to measure spectra with a single detector at a fixed position but with *polychromatic* neutrons and a detector system that can identify the energy of neutrons, e.g., by measuring the time of flight (TOF) of neutrons produced by pulsed spallation on a target. The new TOF neutron diffractometer, HIPPO, at Los Alamos, is dedicated to texture research with 50 detector panels (Fig. 1(a)) that

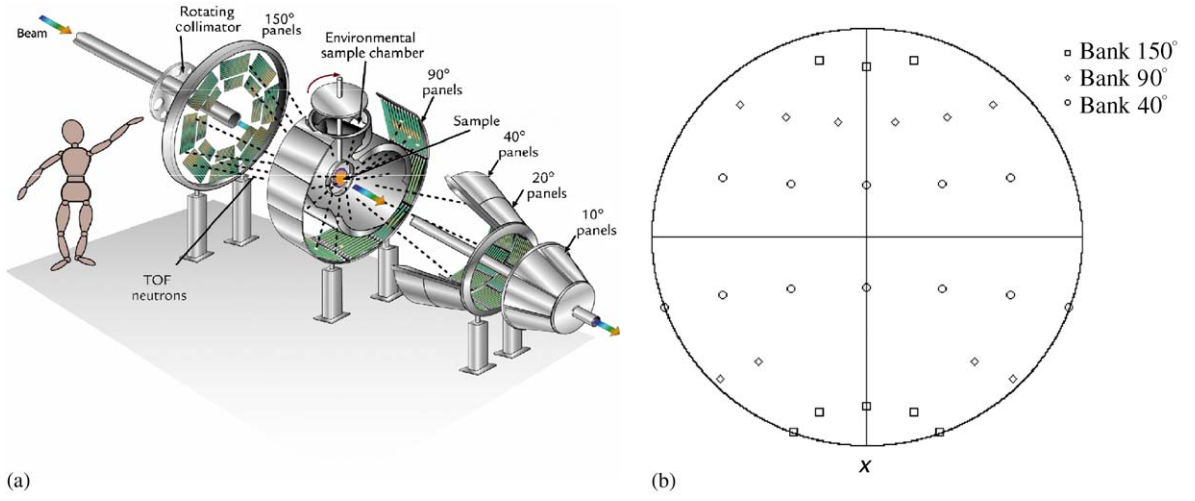

Figure 1
(a) Schematic of the TOF neutron diffractometer HIPPO at Los Alamos National Laboratory. Multiple detector banks are arranged on rings. Each ring (at different 2θ) records reflections of differently oriented lattice planes so that the pole figure is covered simultaneously. A sketch of a (large) person is inserted for scale. (b) Pole figure coverage with thirty $2\theta = 40^\circ$, 90°, and 150° detectors.

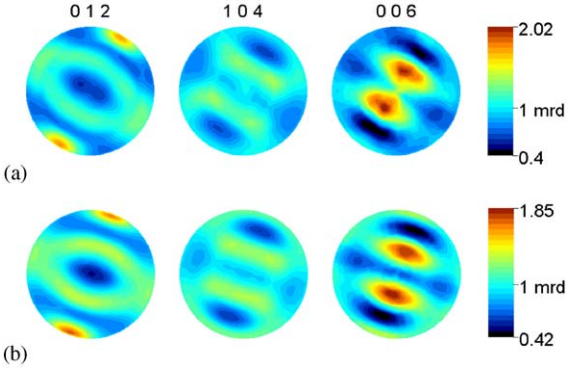

Figure 2
Pole figures for an experimentally deformed limestone round-robin sample measured by neutron diffraction with HIPPO at LANSCE (a) and with D20 at ILL (b). Texture analysis with the Rietveld method, pole figures are equal area projection (Wenk *et al.* 2003).

record simultaneously diffraction spectra from crystals that are in different orientations (Fig. 1(b)) (Wenk *et al.* 2003). Figure 2 shows pole figures for a round-robin sample of experimentally deformed limestone. Results from HIPPO (top) are compared with results obtained with the D20 neutron diffractometer at ILL (bottom). Agreement between the data is excellent; HIPPO data were collected in 1 h while D20 measurements took over 20 h. With these advances neutron texture measurements can document dynamic texture changes, for example, *in situ* during heating through recrystallization and phase transformations.

Local orientations can be measured with the SEM, and this technique is becoming popular because most procedures are automated and do not require much background in texture theory from the user (e.g., Randle and Engler 2000). Electron backscatter diffraction patterns (EBSD or EBSP) taken on small areas ($<1\,\mu m$) are recorded and analyzed by a computer to determine individual orientations. The orientations are then smoothed to provide a continuous ODF. But there are limitations introduced by sample quality, orientation-dependent misindexing artifacts, and statistical considerations. Matthies and Wagner (1996) have explored the relationship between number of measured grains N and the texture strength F_2. (The texture strength is often expressed by the texture index F_2, the integral over the squared ODF.) They established that for large grain numbers, F_2 decreases in a linear fashion with N. This has been illustrated for a sample of anorthosite mylonite, composed of triclinic plagioclase crystals, measured both with neutron diffraction and EBSP (Xie *et al.* 2003). For neutron diffraction, measured on a large volume, the texture index F_2 is 3.1. For EBSP data the texture index descends as a function of grain number (from right to left in Fig. 3). For 400 grains F_2 is 600, for 1000 grains it is 220, and for 5000 grains (the maximum measured in this EBSP experiment) it is still 50. If the linear behavior becomes stable, an extrapolation for infinite N provides the "true" texture coefficient F_2, 3.1, which is closer to the

index determined by neutron diffraction. The "true" texture strength can be obtained by smoothing discrete data, for example, with a Gauss filter or harmonic functions, but the width of the filter function is not known *a priori*; it depends on the texture type, the texture strength, and the number of measured data points. In the case of the anorthosite illustrated in Fig. 3, the appropriate Gauss filter is 18°. Naturally, for geophysicists concerned with physical properties of rocks, a quantitative characterization is important and arbitrary smoothing is inadequate.

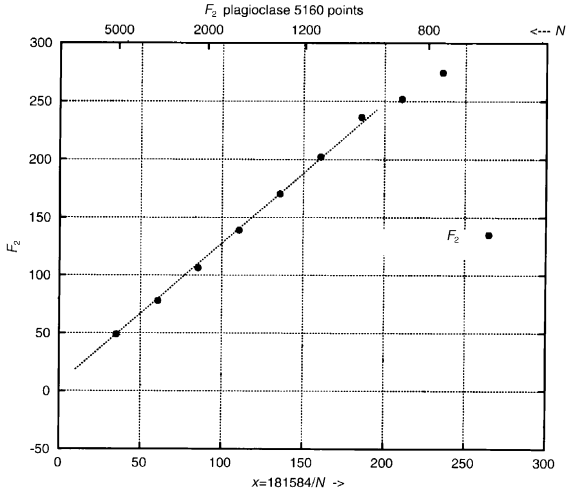

Figure 3
Dependence of the texture strength, described by the texture index F_2, on the number of orientations measured by EBSD, for the case of plagioclase. The "true" texture index, established by neutron diffraction measurements on the same sample is 3.2. Shown is the dependence of F_2 upon the number N of orientations (Xie *et al.* 2003).

The unique advantages of high-intensity, small beam size (< 5 μm), and free choice of wavelength for synchrotron x-rays opens a wide range of new possibilities (e.g., Heidelbach *et al.* 1999, Wcislak *et al.* 2002, Wenk and Grigull 2003). Synchrotron diffraction images, recorded by CCD detectors, almost instantaneously display the presence of texture expressed in systematic intensity variations along Debye rings (Fig. 4(a)). This is particularly significant for *in situ* high-pressure studies of textures with diamond anvil cells (e.g., Merkel *et al.* 2002). Diamond anvil cells have been used to investigate high-pressure phase relations and establish equilibrium temperature–pressure phase diagrams, investing great efforts to achieve a hydrostatic environment of the sample. But a diamond cell can also be used to exert stress and to deform the sample at high pressure. With a radial geometry (Fig. 4(b)) texture changes during deformation can be observed *in situ*. The directional stress component produces both elastic and plastic deformation. Elastic deformation is visible in peak shifts along the Debye ring (Fig. 5) and can be used to assess elastic properties of minerals (e.g., Singh *et al.* 1998, Matthies *et al.* 2001). Plastic deformation and texture development are expressed in intensity variations along a Debye ring.

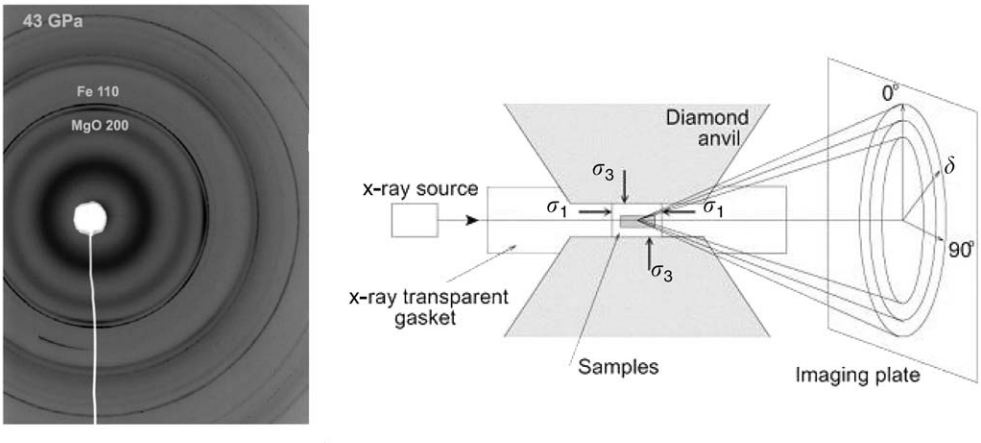

Figure 4
Synchrotron x-ray diffraction diamond anvil experiment in transmission. (a) A diffration image with Debye rings of MgO and Fe measured at 40 GPa pressure. (b) Geometry of the radial diffraction experiment, used to deform samples at very high pressure and measure the development of preferred orientation and lattice strain *in situ* (Merkel *et al.* 2002).

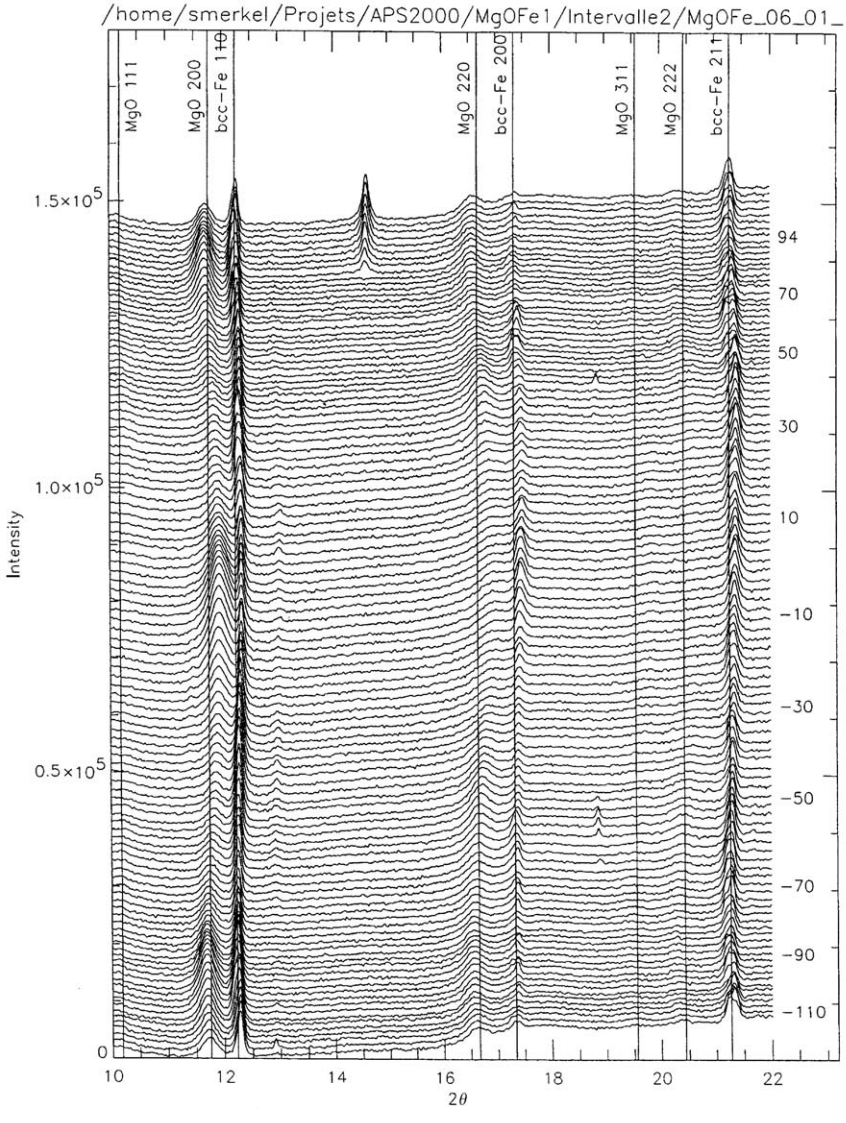

Figure 5
The processed image of Fig. 3 showing a stack of diffraction patterns at different orientations to the compression direction. The changes in intensity document presence of texture due to plastic deformation, the shifts of diffraction peaks indicate elastic deformation under stress (Merkel *et al.* 2002).

Diamond anvil cells are limited by the small sample volume that requires small grain size, and such deformation experiments are not adequate to investigate size-dependent mechanisms (e.g., Wang 1994). Larger volumes can be obtained in modified multi-anvil apparatus (Durham *et al.* 2002), yet such deformation experiments have not been applied to *in situ* texture research and are not possible at extreme pressures (>30 GPa).

3. Data Analysis

A few comments ought to address issues of data analysis. As is metallurgy the texture of geological materials is described with the ODF. Knowledge about the ODF is required to determine physical tensor properties of polycrystals. The main difference to metals is that most minerals have low crystal symmetry and most rock samples have low sample

symmetry and this leads to modified approaches. Experimental texture data have various forms. With electron microscopes and the universal stage petrographic microscope, single orientations are measured. This has the advantage that an ODF can be determined directly and unambiguously by entering orientations into the ODF. However, it requires adequate smoothing and normalization. If pole figures of certain lattice planes (*hkl*) are measured, then it is more difficult to retrieve the ODF and there is some inherent ambiguity.

There are various methods to retrieve the three-dimensional ODF from measured two-dimensional pole figures (for a review see Kallend 2000). One set of methods works in direct space and uses algorithms of tomography. The Williams–Imhof–Matthies–Vinel (WIMV) method, introduced by Matthies and Vinel (1982), the arbitrarily defined cells (ADCs) (Pawlik *et al.* 1991), and the maximum entropy method (Liang *et al.* 1988, Schaeben 1988) are most widely used. Other methods work in Fourier space, most notably the harmonic method introduced by Bunge (1965) and Roe (1965). The harmonic method is elegant for highly symmetric textures (such as cubic crystal and orthorhombic sample symmetry), because it can take advantage of the symmetrized harmonic functions. For lower symmetries it is increasingly awkward. There are several software packages that calculate ODFs from pole figures for all crystal and sample symmetries, and perform other operations to quantify textures in polycrystals (e.g., BEARTEX, Wenk *et al.* 1998; LaboTex, Pawlik *et al.* 1991; MulTex, Helming 1994; POPLA, Kallend *et al.* 1991, TexTools, Resmat Corp.). Details can be obtained from the Internet.

Traditionally, texture analysis has relied on pole figure measurements. This is efficient if only a few pole figures are required for the ODF analysis and if diffraction peaks are reasonably strong (relative to background) and well separated. The method becomes increasingly unsatisfactory for complex diffraction patterns of polyphase materials and low-symmetry compounds with many closely spaced and partially or completely overlapped peaks, as is the case for many minerals.

Another approach is to use many pole figures and few sample orientations. This is an obvious advantage for TOF neutron diffraction where many diffraction peaks are measured in a continuous spectrum. Pole figures can be considered as two-dimensional projections of the ODF (Fig. 6). Each diffraction peak intensity in a spectrum is a one-dimensional projection. To determine the ODF value of a cell, three projection paths have to intersect. Texture analysis from diffraction spectra can take advantage of the Rietveld (1969) method of crystallography, and obtain the ODF either with Fourier or with direct methods. The finite number of harmonic ODF coefficients can be refined in a similar way as crystallographic parameters with a nonlinear least-squares procedure (Von Dreele 1997). With discrete methods ODF values are directly related to peak intensity values in the spectra (Lutterotti *et al.* 1997). The Rietveld method has been applied to several mineral textures, including calcite (Lutterotti *et al.* 1997, Von Dreele 1997), eclogite (Wenk *et al.* 2001), and plagioclase (Xie *et al.* 2003). The method is implemented in software packages GSAS and MAUD. Pole figures shown in Fig. 2 were extracted from neutron diffraction spectra with the Rietveld method.

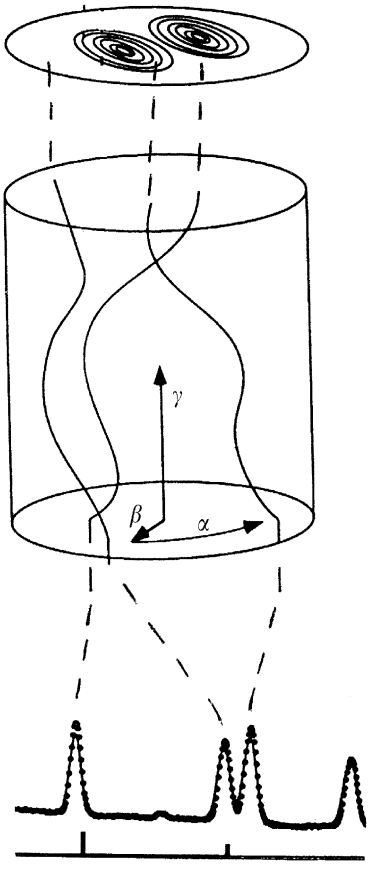

Figure 6
The three-dimensional orientation distribution of Euler angles can be viewed as a probability distribution in cylindrical space of angles α (azimuth in sample coordinates), β (pole distance), and γ (azimuth in crystal space). A pole figure is a two-dimensional projection of the ODF; a peak intensity in a diffraction pattern is proportional to a one-dimensional projection.

For geophysicists, aggregate physical properties are of interest. These properties depend on crystal orientation, compositional layering, open fractures,

or partial melt (Crampin 1981). In a rock with oriented fractures, seismic waves travel much faster parallel to fractures than across them, but with increasing pressure, fractures close and their influence on anisotropy diminishes (e.g., Kern 1993). If we know the ODF and single-crystal physical properties, we can calculate the influence of single crystals on the polycrystal physical properties. Elastic properties, on which seismic, wave propagation depends, are described as a fourth rank tensor. Single-crystal elastic constants for many minerals under a variety of conditions have been compiled (e.g., Simmons and Wang 1971). Polycrystal elastic properties are obtained by a summation over all contributing single crystals. If there is preferred orientation, a macroscopic anisotropy for the aggregate will result. The summation should maintain continuity across grain boundaries when a stress is applied, and minimize local stress concentrations. In practice, the local stress and strain distribution is usually neglected and the summation is done by simple averages. There are two extreme cases: The Voigt average assumes constant strain throughout the material. The Reuss average assumes that stress is constant. There are other averages that are intermediate between constant strain and constant stress. One example is the Hill (1952) average, an arithmetic mean of Voigt and Reuss averages, or the geometric mean (Matthies and Humbert 1993).

4. Polycrystal Plasticity Simulations

Texture patterns are used by geologists to infer the deformation history. One of the universal principles of texture interpretation is symmetry and it has been widely applied to geological situations: The texture symmetry cannot be lower than the symmetry of the strain path (Paterson and Weiss 1961), if it started out uniform. For coaxial deformation one expects orthorhombic pole figures, whereas a noncoaxial path is likely to produce monoclinic pole figures. More detailed interpretations rely on comparisons of observed textures with plasticity simulations.

In engineering, simulations are performed because they are easier than costly experiments. In Earth science it is often not possible to reproduce the complex strain paths or the high-pressure, high-temperature, slow strain rate conditions that occur in nature. If microscopic mechanisms that are active under a given set of conditions are known and if a good constitutive theory exists, then the polycrystal behavior for any strain path can be simulated, including, for example, heterogeneous subduction of slabs to the bottom of the Earth's mantle.

Different mechanisms can produce or modify texture. Most important is dislocation glide, which we will discuss in some detail in the next section. Also significant is recrystallization, either dynamic or static, with nucleation of new domains and grain-boundary mobility. Textures may be inherited during phase transformations. If fluids are present, aspects of dissolution and growth in a stress field can have a profound influence on resulting orientation patterns (e.g., Spiers and Takeshita 1995, Bons and den Brok 2000). Particularly for fine-grained aggregates, grain-boundary sliding may occur.

Deformation of a polycrystal is a very complicated heterogeneous process. When an external stress is applied to the polycrystal, it is transmitted to individual grains. Dislocations move on slip systems, dislocations interact and cause "hardening," grains change their shape and orientation, thereby interacting with neighbors and creating local stresses that need to be accommodated. This can result in very heterogeneous microstructures such as in a granitic mylonite with highly deformed softer quartz grains and more angular fragments of stronger feldspar (Fig. 7). Modeling these processes is a formidable task and only recently have three-dimensional finite element formulations been developed to capture at least some aspects for cubic metals (Mika and Dawson 1999). The difficulty is that in real materials local stress equilibrium and local strain continuity are approximated, and this requires heterogeneity at the microscopic level. Most of the polycrystal plasticity simulations have used highly simplistic approximations. For rocks, a variety of models have been applied, ranging from empirical assumptions to sophisticated theories. It has been assumed that slip directions align along flow lines (e.g., Hess 1965). With continuum mechanics, deformation of crystals can be predicted (e.g., Ribe and Yu 1991). The

Figure 7
Microstructure of a highly deformed granite from the Bergell Alps. Quartz deforms ductiles and grains are bent and flattened. Feldspar undergoes brittle deformation with large crystals fragmented into angular blocks. Image taken with a petrographic microscope and crossed polarizers.

standard methods used in metallurgy were applied such as compatibility (e.g., Lister *et al.* 1978), equilibrium (e.g., Dawson and Wenk 2000), and self-consistent methods (e.g., Wenk 1999). Most recently, finite element method (FEM) models were used (Lebensohn *et al.* 2003). All provided some useful results and approximations that helped seismologists to better understand anisotropy.

Earth materials differ from metals in some respects. Minerals have a high strain rate sensitivity (low stress exponent; 3–9 versus >99 in metals) and differently oriented crystals may deform at very different rates. Minerals have lower symmetry and thus fewer equivalent slip systems. This causes a high plastic anisotropy and some orientations deform much more than others. Both features suggest that deformation of mineral aggregates is heterogeneous and this has to be taken into account in models.

The Taylor (1938) model, suggesting that straining could be partitioned equally among all crystals and thus maintaining compatibility across grain boundaries, is of limited applicability in plastically highly anisotropic minerals. For this approach even to be viable, each individual crystal must be able to accommodate an arbitrary deformation, requiring five independent slip systems. Using the Taylor model for minerals with few slip systems can lead to prediction of excessively high stresses, incorrect texture components, or both.

Contrary to the Taylor hypothesis, all crystals in a polycrystal can be required to exhibit identical stress (equilibrium), given that their behavior is rate dependent at the slip system level. This is a variant of the original Sachs (1928) assumption for rate-independent behavior in which the stresses in the crystals throughout an aggregate share a common direction. The equal stress hypothesis is more effective for polycrystals comprised of crystals with fewer than five slip systems. The principal drawback is that deformation often is concentrated too highly in a small number of crystals, leading to inaccurate texture predictions. With the Sachs approach only the most favorable slip systems are activated and, therefore, stresses are low.

Other approaches have been developed to take into account heterogeneous deformation of highly anisotropic polycrystals. For example, Molinari *et al.* (1987) developed the viscoplastic self-consistent (VPSC) formulation for large strain deformation in which each grain is regarded as an inclusion embedded in a viscoplastic homogeneous equivalent medium whose properties coincide with the average properties of the polycrystal. A more general formulation with an anisotropic medium was introduced by Lebensohn and Tomé (1993). The VPSC method has been applied to several mineral systems (see review by Wenk 1999).

Simple shear texture simulations for olivine illustrate that overall results for Taylor (Fig. 8(a)) and VPSC (Fig. 8(b)) are similar, but there are significant differences that are best seen by following rotations of individual grains (Figs. 8(c) and 8(d)). Grain A is initially oriented with [100] perpendicular to the shear plane and grain B with [100], the preferred slip direction, parallel to the macroscopic shear direction. For Taylor, grain B deforms by shear deformation homogeneously and thus does not rotate, while for VPSC, the grain environment imposes strains that rotate [100] against the sense of shear.

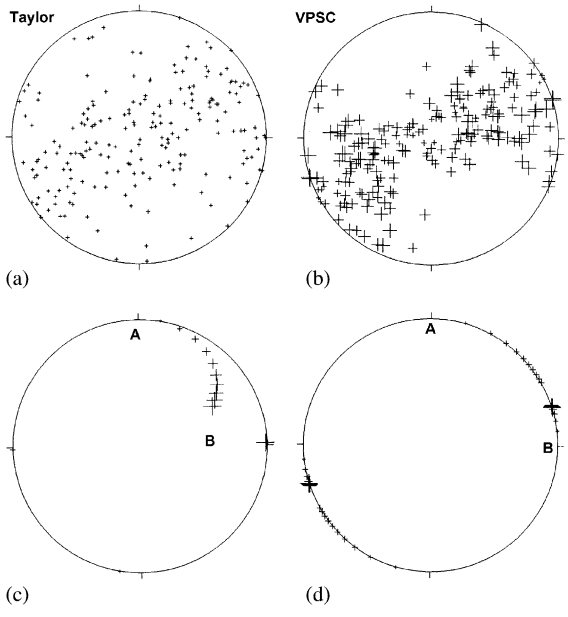

Figure 8
Deformation of an olivine in simple shear, simulated with the Taylor model (a, c) and the self-consistent theory (b, d). [100] pole figures represented in equal area projection, shear plane is horizontal, shear direction is E–W. (a, b) Orientations of 500 initially randomly oriented grains. (c, d) Rotation trajectories of two grains, A and B. Size of symbols is proportional to the relative deformation (Wenk and Tome 2000).

With FEMs local heterogeneity can be taken into account. Every grain is either discretized with a single element (Sarma and Dawson 1996) or with many elements (Mika and Dawson 1999). The deformation of a grain depends both on its orientation and the orientations of neighbors. FEM has recently been applied to halite (Lebensohn *et al.* 2003), a cubic mineral, but plastically highly anisotropic because the favored slip system $\{110\}\langle 11-0\rangle$ has only two independent variants and harder slip systems are required to deform an aggregate homogeneously. Differences between the models are best visible in the grain shape distribution as illustrated for d_{12} strain rate components in Fig. 9. For homogeneous

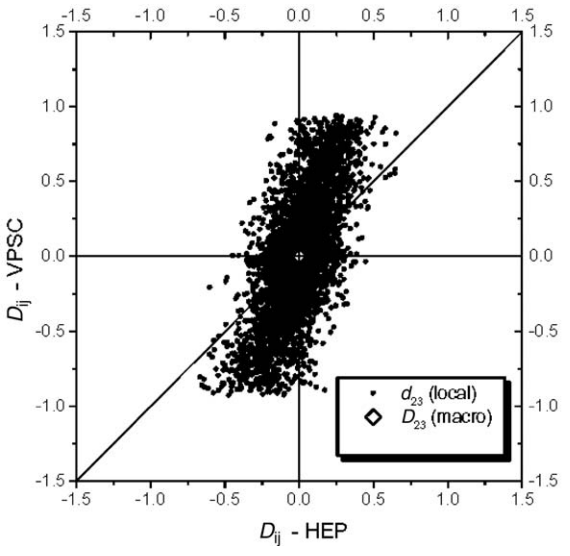

Figure 9
Polycrystal plasticity simulations for halite. Shown are the off diagonal strain rate components d_{12} predicted at the initial step of each simulation. For Taylor assumption all grains deform at the same rate (dot in center), for VPSC there is a large spread, and for FEM (HEP for Hybrid Element Polycrystal) there is a moderate spread (Lebensohn *et al*. 2003).

deformation (Taylor) all grains have the same strain rate (circle in center). For VPSC there is a very large spread, some grains deforming over 10 times more than others. For FEM, the spread is considerably smaller and similar to that which is actually observed.

It must be emphasized that texture is the result of the accumulated strain history, which is particularly significant for geological situations where the strain path often varies. In simulations such changes can be easily included and texture evolution, for example, in a highly heterogeneous system, such as a convection cell in the Earth's mantle, can be simulated (e.g., Dawson and Wenk 2000).

The relationship between slip and crystal rotations is straightforward. Other processes such as climb, grain-boundary sliding, diffusion in general may also affect orientation distributions. Of particular importance in geological situations is recrystallization.

For metamorphic petrologists, recrystallization means growth of new mineral assemblages to attain thermodynamic equilibrium in different temperature and pressure conditions. In deformation studies, recrystallization is the development of strain-free regions, either during deformation (dynamic recrystallization; Guillopé and Poirier 1979) or after deformation (static recrystallization). More highly deformed grains have a higher strain energy than less deformed grains. Those grains may be consumed through boundary migration by less deformed grains (growth). Alternatively, dislocation-free nuclei may form in highly deformed grains and then grow at the expense of others. If growth is controlling, "hard" grains with little deformation dominate the texture and highly deformed grains will disappear. If nucleation is prevalent, "soft" grains develop nuclei that will ultimately grow and dominate the fabric. In order for a boundary to become mobile, there is also a requirement for a significant misorientation. In geological materials recrystallization is often evident as grain-size reduction (e.g., Drury and Urai 1990). This may be due to nucleation that often initiates along grain boundaries and twins, or it may be due to subgrain formation during recovery that can produce large misorientations. The importance of changes in grain-size distribution during recrystallization has been analyzed by Shimizu (1999).

Recrystallization thus can alter the texture pattern not through generation of new orientations but through selection of certain orientation components. A simple model for such selection was proposed by Jessell (1990), evaluating grain deformation with the Taylor model. Heterogeneous orientation-dependent deformation can be more rigorously approached with the self-consistent theory, and this was the basis for

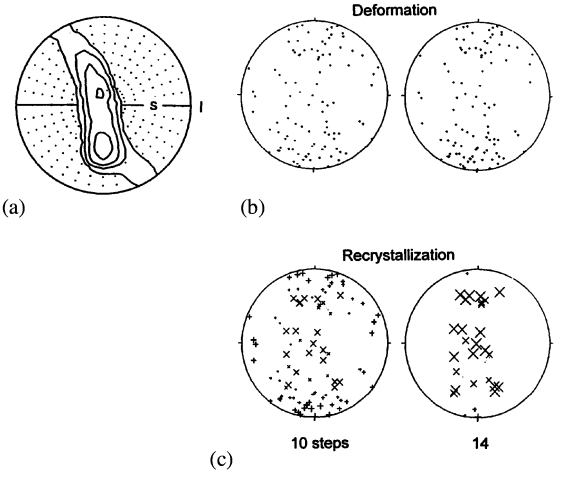

Figure 10
VPSC simulations of texture changes during deformation and recrystallization of quartz in pure shear plane strain. (0001) $=c$ pole figures, shortening direction is vertical, extension direction horizontal. (a) Typical texture of naturally deformed and dynamically recrystallized quartzite. (b) Texture development during deformation. (c) Texture development id deformation is accompanied by recrystallization with significant nucleation. Symbol size is proportional to grain size, + symbols denote old grains, × symbols newly nucleated grains (Wenk 2000).

modeling texture changes by balancing grain growth and nucleation (Wenk *et al.* 1997). Deformation simulations with the self-consistent model provide a population of grains with a variation in deformation and correspondingly in dislocation density. The microstructural hardening of slip systems during deformation provides an incremental strain energy to grains after each deformation step. In the model the stored energy of each grain is compared with the average stored energy of the polycrystal. If the stored energy of a grain is lower than the average, it grows; if it is higher, it shrinks. A grain may disappear. If nucleation of strain-free domains accompanies boundary migration, a highly deformed parent grain divides upon reaching a threshold strain rate and produces an undeformed nucleus. The nucleus takes on the current orientation of the parent at the time of its formation, but its strain is reset to zero. This has an effect on the subsequent evolution, because these strain-free domains can grow much faster. In this case highly deformed grains dominate the final texture.

Results are illustrated for recrystallization of quartz. A typical quartz texture observed in metamorphic quartzites is shown in Fig. 10(a) . It shows a broad $c = (0001)$ maximum in the schistosity plane (s) perpendicular to the lineation (l) direction. It is impossible to obtain this maximum for pure deformation. The *c*-axes tend to be oriented perpendicular to the schistosity plane (Fig. 10(b)). If recrystallization accompanies deformation, the highly deformed grains in the center of the pole figure nucleate ($\times$ symbols) and grow, increasingly replacing the less deformed old grains ($+$ symbols, Fig. 10(c)).

The recrystallization model was successfully used to simulate static and dynamic recrystallization textures in geologic materials such as quartz (Takeshita *et al.* 1999), calcite (Lebensohn *et al.* 1998), and olivine (Wenk and Tomé 1999). A similar approach was applied by Thorsteinsson (2001, 2002) to ice, and by Kaminski and Ribe (2001) to olivine. All these approaches are highly simplistic to the complex and still poorly understood process of recrystallization, but they provide methods to investigate possible changes in bulk anisotropy during recrystallization.

How sensitive are the various model assumptions for the broader picture of seismic anisotropy in the Earth? This was recently explored by Blackman *et al.* (2001) for upwelling of mantle material along a ridge. Figure 11 illustrates olivine texture patterns along a streamline produced with the lower bounds model, the VPSC theory, recrystallization with dominating growth and recrystallization with dominating

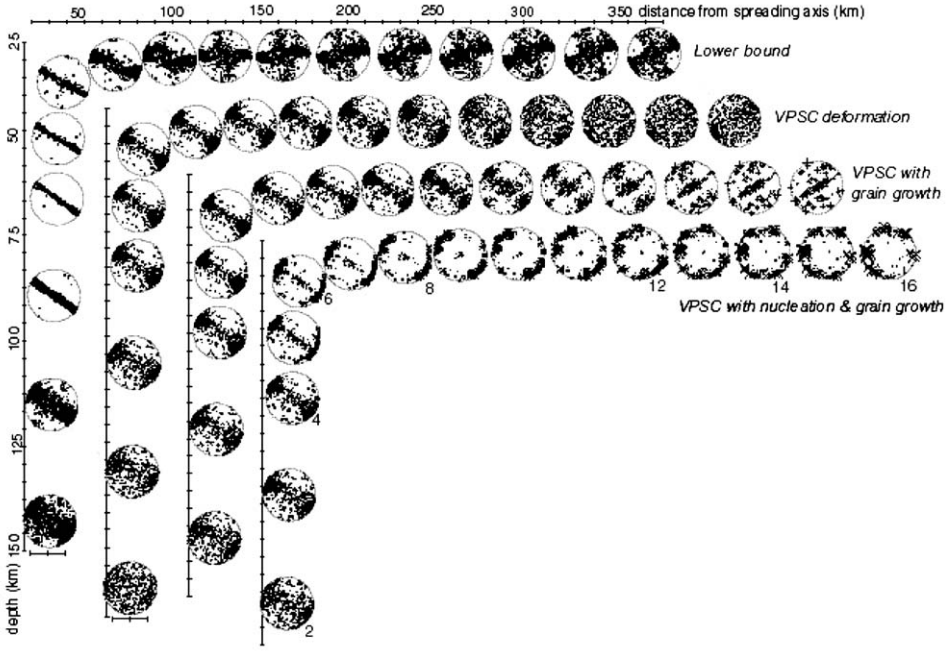

Figure 11
[100] pole figures for olivine simulated for mantle upwelling near a ridge. Results for different plasticity models are compared. From left to right: lower bounds model, self-consistent deformation model, self-consistent deformation accompanied by growth-favored dynamic recrystallization, self-consistent deformation accompanied by balanced nucleation and growth dynamic recrystallization (Blackman *et al.* 2002).

nucleation. The texture patterns vary in detail but are overall quite similar, particularly when elastic properties are calculated by averaging. Obviously, in the future the models will become refined to take more of the detailed mechanisms and constraints into account. This example serves as a link to advance to Part II and apply some of the methods described here to investigate texture development in the deep Earth.

Bibliography

Blackman D K, Wenk H-R, Kendall J-M 2002 Seismic anisotropy in the upper mantle: 1. Factors that affect mineral texture and effective elastic properties. *Geochem. Geophys. Geosys.* **3**, 10.1029

Bons P D, Den Brok B 2000 Crystallographic preferred orientation development by dissolution–precipitation creep. *J. Struct. Geol.* **22**, 1713–22

Bunge H-J 1965 Zur Darstellung allgemeiner Texturen. *Z. Metallk.* **56**, 872–4

Bunge H-J (ed.) 1986 *Experimental Techniques of Texture Analysis*. DMG Informationsgemeinschaft, Oberursel, Germany, 442pp.

Crampin S 1981 A review of wave motion in anisotropic and cracked elastic media. *Wave Motion* **3**, 242–391

D'Halloy O J J 1833 *Introduction à la Géologi*e. Levrault, Paris, 894pp.

Dawson P R, Wenk H-R 2000 Texturing of the upper mantle during convection. *Phil. Mag. A* **80**, 573–98

Drury M R, Urai J L 1990 Deformation-related recrystallization processes. *Tectonophysics* **172**, 235–53

Durham W B, Weidner D J, Karato S-Y, Wang Y 2002 New developments in deformation experiments at high pressure. In Karato S-I, Wenk H-R (eds.) *Plastic Deformation in Minerals and Rocks*, Reviews in Mineralogy. Mineralogical Society of America, Vol. 51. pp. 21–49

Guillopé M, Poirier J-P 1979 Dynamic recrystallization during creep of single-crystalline halite: an experimental study. *J. Geophys. Res.* **84**, 5557–67

Heidelbach F, Riekel C, Wenk H-R 1999 Quantitative texture analysis of small domains with synchrotron x-rays. *J. Appl. Cryst.* **32**, 841–9

Helming K 1994 Some applications of the texture component method. In: *Proc. 10th Int. Conf. on Texture of Materials*, Clausthal. Materials Science Forum, Vol. 157–162, pp. 363–8

Hess H H 1964 Seismic anisotropy of the uppermost mantle under oceans. *Nature* **203**, 629

Hill R 1952 The elastic behavior of a crystalline aggregate. *Proc. Phys. Soc.* **A65**, 349–54

Jessel M W 1988 Simulation of fabric development in recrystallizing aggregates: I. Description of the model. *J. Struct. Geol.* **10**, 771–8

Kallend J S 2000 Determination of the orientation distribution from pole figure data, Chapter 3 in *Texture and Anisotropy*. In: Kocks U F, Tomé C N, Wenk H-R (eds.), *Preferred Orientations in Polycrystals and Their Effect on Materials Properties*, 2nd Paperback edn. Cambridge University Press, 102–24

Kallend J S, Kocks U F, Rollett A D, Wenk H-R 1991 Operational texture analysis. *Mater. Sci. Eng.* **A132**, 1–11

Kaminski E, Ribe N M 2001 A kinematic model for recrystallization and texture development in olivine polycrystals. *Earth Planet. Sci. Lett.* **189**, 253–67

Karato S-I, Wenk H-R 2002 *Plastic Deformation in Minerals and Rocks*. Reviews in Mineralogy. Mineralogical Society of America. Vol. 51. 420pp.

Kern H 1993 P- and S-wave anisotropy and shear wave splitting at pressure and temperature in possible mantle rocks and their relation to the rock fabric. *Phys. Earth. Planet. Inter.* **78**, 245–56

Kocks U F, Tomé C N, Wenk H-R (eds.) 2000 *Texture and Anisotropy. Preferred Orientations in Polycrystals and their Effect on Materials Properties*, 2nd Paperback edn. Cambridge University Press, 676pp.

Lebensohn R A, Tomé C N 1993 A self-consistent anisotropic approach for the simulation of plastic deformation and texture development of polycrystals—application to zirconium alloys. *Acta Metall. Mater.* **41**, 2611–24

Lebensohn R A, Wenk H-R, Tomé C 1988 Modelling deformation and recrystallization textures in calcite. *Acta Mater.* **46**, 2683–93

Lebensohn R A, Dawson P R, Wenk H-R, Kern H M 2003 Heterogeneous deformation and texture development in halite: modelling with finite element and self-consistent approaches, and experimental validation. *Tectonophysics* (in press)

Liang Z, Wang F, Xu J 1988 Inverse pole figure determination according to the maximum entropy method. In: Kallend J S, Gottstein G (eds.) *Eighth Int. Conf. on Textures of Materials*. The Metallurgical Society, Warrendale, PA, pp. 111–14

Lister G S, Paterson M S, Hobbs B E 1978 The simulation of fabric development during plastic deformation and its application to quartzite: the model. *Tectonophysics* **45**, 107–58

Lutterotti L, Matthies S, Wenk H-R, Schultz A J, Richardson J W 1997 Combined texture and structure analysis of deformed limestone from time-of-flight neutron diffraction spectra. *J. Appl. Phys.* **81**, 594–600

Matthies S, Humbert M 1993 The realization of the concept of the geometric mean for calculating physical constants of polycrystalline materials. *Phys. Stat. Sol. (b)* **177**, K47–50

Matthies S, Vinel G W 1982 On the reproduction of the orientation distribution function of textured samples from reduced pole figures using the concept of conditional ghost correction. *Phys. Stat. Sol. (b)* **112**, K111–14

Matthies S, Wagner F 1996 On a $1/n$ law in texture related single orientation analysis. *Phys. Stat. Sol. (b)* **196**, K11–15

Matthies S, Merkel S, Wenk H-R, Hemley R J, Mao H-K 2001 Effects of texture on the determination of elasticity of polycrystalline ε-iron from diffraction measurements. *Earth Planet. Sci. Lett.* **194**, 201–12

Merkel S, Wenk H-R, Shu J, Shen G, Gillet P, Mao H-K, Hemley R J 2002 Deformation of MgO aggregates at pressures of the lower mantle. *J. Geophys. Res.* **107**(B11), 2271, ECV3, 1–17

Mika D P, Dawson P R 1999 Polycrystal plasticity modeling of intracrystalline boundary textures. *Acta Mater.* **47**, 1355–69

Molinari A, Canova G R, Ahzi S 1987 A self-consistent approach of the large deformation polycrystal viscoplasticity. *Acta Metall.* **35**, 2983–94

Paterson M S, Weiss L E 1961 Symmetry concepts in the structural analysis of deformed rocks. *Geol. Soc. Am. Bull.* **72**, 841–82

Pawlik K, Pospiech J, Lücke K 1991 The ODF approximation from pole figures with the aid of the ADC method. *Textures Microstruct.* **14–18**, 25–30

Phillips W R 1971 *Mineral Optics, Principles and Techniques*. Freeman, San Francisco, 249pp.

Randle V, Engler O 2000 *Introduction to Texture Analysis: Macrotexture, Microtexture and Orientation Mapping*. Gordon and Breach

Reuss A 1929 Berechnung der Fliessgrenze von Mischkristallen auf Grund der plastizitätsbedingung für Einkristalle. *Z. Angew. Math. Mech.* **9**, 49–58

Ribe N, Yu Y 1991 A theory for plastic deformation and textural evolution of olivine polycrystals. *J. Geophys. Res.* **96**, 8325–35

Rietveld H M 1969 A profile refinement method for nuclear and magnetic structures. *J. Appl. Cryst.* **2**, 65–71

Roe R-J 1965 Description of crystallite orientation in polycrystalline materials: III. General solution to pole figure inversion. *J. Appl. Phys.* **36**, 2024–31

Sachs G 1928 Zur Ableitung einer Fliessbedingung. *Z. Ver. Dtsch. Ing.* **72**, 734–6

Sander B 1950 *Einführung in die Gefügekunde der Geologischen Körper*. Springer, Vienna, Vol. 2, 409pp.

Sarma G B, Dawson P R 1996 Effects of interaction among crystals on the inhomogeneous deformations of polycrystals. *Acta Mater.* **44**, 1937–53

Schaeben H 1988 Entropy optimization in texture goniometry. *Phys. Stat. Sol. (b)* **148**, 63–72

Schulz L G 1949 A direct method of determining preferred orientation of a flat transmission sample using a geiger counter x-ray spectrometer. *J. Appl. Phys.* **20**, 1030–3

Shimizu I 1999 A stochastic model of grain size distribution during dynamic recrystallization. *Phil. Mag. A* **79**, 1217–31

Simmons G, Wang H, 1971 *Single Crystal Elastic Constants and Calculated Aggregate Properties: A Handbook*, 2nd edn. The MIT Press, 370pp.

Singh A K, Mao H-K, Shu J, Hemley R J 1998 Estimation of single-crystal elastic moduli from polycrystalline x-ray diffraction at high pressure: application to FeO and iron. *Phys. Rev. Lett.* **80**, 2157–60

Snyder R L, Fiala J, Bunge H-J (eds.) 1999 *Defect and Microstructure Analysis by Diffraction*, IUC Monogr. on Crystallography 10. Oxford University Press, 785pp.

Spiers C J, Takeshita T (eds.) 1995 Influence of fluids on pressure solution in rocks. *Tectonophysics* **245** (special issue)

Takeshita T, Wenk H-R, Lebensohn R 1999 Development of preferred orientation and microstructure in sheared quartzite: comparison of natural and simulated data. *Tectonophysics* **312**, 133–55

Taylor G I 1938 Plastic strain in metals. *J. Inst. Metals* **62**, 307–24

Thorsteinsson T 2001 An analytical approach to deformation of anisotropic ice-crystal aggregates. *J. Glaciol.* **47**, 507–16

Thorsteinsson T 2002 Fabric development with nearest-neighbor interaction and dynamic recrystallization. *J. Geophys. Res.* **107**, 148–227

Voigt W 1928 *Lehrbuch der Kristallphysik*. Teubner, Leipzig, 978pp.

Von Dreele R B 1997 Quantitative texture analysis by rietveld refinement. *J. Appl. Cryst.* **30**, 517–25

Wang J N 1994 The effect of grain size distribution on the rheological behavior of polycrystalline materials. *J. Struct. Geol.* **16**, 961–70

Wcislak L, Klein H, Bunge H-J, Garbe U, Tschentscher T, Schneider J R 2002 Texture analysis with high-energy synchrotron radiation. *J. Appl. Cryst.* **35**, 82–95

Wenk H-R (ed.) 1985 *Preferred Orientation in Deformed Metals and Rocks. An Introduction to Modern Texture Analysis*. Academic Press, 610pp.

Wenk H-R 1999 A voyage through the deformed earth with the self-consistent model. *Model. Mater. Sci. Eng.* **7**, 699–722

Wenk H-R, Grigull S 2003 Synchrotron texture analysis with area detectors. *J. Appl. Cryst.* (in press)

Wenk H-R, Tomé C N 1999 Modeling dynamic recrystallization of olivine aggregates deformed in simple shear. *J. Geophys. Res.* **104**, 25513–27

Wenk H-R, Canova G, Brechet Y, Flandin L 1997 A deformation-based model for recrystallization of anisotropic materials. *Acta Mater.* **45**, 3283–96

Wenk H-R, Matthies S, Donovan J, Chateigner D 1998 BEARTEX, a Windows-based program system for quantitative texture analysis. *J. Appl. Cryst.* **31**, 262–9

Wenk H-R, Cont L, Xie Y, Lutterotti L, Ratschbacher L, Richardson J 2001 Rietveld texture analysis of dabie shan eclogite from TOF neutron diffraction spectra. *J. Appl. Cryst.* **34**, 442–53

Wenk H-R, Lutterotti L, Grigull S, Vogel S 2003 Texture analysis with the new HIPPO TOF diffractometer. *Nucl. Instr. Methods A* (in press)

Xie Y, Wenk H-R, Matthies S 2003 Plagioclase preferred orientation by TOF neutron diffraction and SEM-EBSD. *Tectonophysics* (in press)

H.-R. Wenk

Encyclopedia of Materials: Science and Technology
ISBN: 0-08-043152-6
pp. 1–11